

Agrowaste-Based Nanofibers as a Probiotic Encapsulant: Fabrication and Characterization

Wai-Yee Fung,[†] Kay-Hay Yuen,[†] and Min-Tze Liong^{*,‡}

[†]School of Pharmaceutical Sciences and [‡]School of Industrial Technology, Universiti Sains Malaysia, 11800 Penang, Malaysia

ABSTRACT: This study explored the potential of soluble dietary fiber (SDF) from agrowastes, okara (soybean solid waste), oil palm trunk (OPT), and oil palm frond (OPF) obtained via alkali treatment, in the nanoencapsulation of *Lactobacillus acidophilus*. SDF solutions were amended with 8% poly(vinyl alcohol) to produce nanofibers using electrospinning technology. The spinning solution made from okara had a higher pH value at 5.39 ± 0.01 and a higher viscosity at 578.00 ± 11.02 mPa·s ($P < 0.05$), which resulted in finer fibers. FTIR spectra of nanofibers showed the presence of hemicellulose material in the SDF. Thermal behavior of nanofibers suggested possible thermal protection of probiotics in heat-processed foods. *L. acidophilus* was incorporated into the spinning solution to produce nanofiber-encapsulated probiotic, measuring 229–703 nm, visible under fluorescence microscopy. Viability studies showed good bacterial survivability of 78.6–90% under electrospinning conditions and retained viability at refrigeration temperature during the 21 day storage study.

KEYWORDS: agrowaste, oil palm, okara, nanofibers, electrospinning, *Lactobacillus*, probiotic, nanoencapsulation

INTRODUCTION

Oil palm and soybean are the two largest oil crop commodities in the world, both cumulatively contributing more than half of the world's total oil production of 163.9 million tonnes in 2009.¹ Indonesia and Malaysia are the largest oil palm producers, whereas the United States and Brazil are the largest producers of soybean.¹ However, the expansion of these commodities is resulting in overproduction of biomass wastes, because only a small fraction of the plants is commercially valuable. Up to 90% of the oil palm is constituted of oil palm trunk (OPT) and oil palm frond (OPF), among other fibrous wastes, which contain lignin, cellulose, and hemicelluloses. Okara is the main solid waste from soy- and tofu-processing industries, which contains up to 49% total dietary fiber.² In view of sustainable development, there is aggressive research in transforming the high-volume wastes which cause disposal and environmental problems to natural resources for the production of sustainable products, such as liquid biofuel,³ fertilizer, fodder, and even human food products.⁴

Increasing awareness in health and nutrition has promoted consumption of dietary supplements and nutraceuticals to improve health. Probiotics are viable gut microorganisms, which symbiotically exert beneficial effects to the host's physiology when ingested and sustained in adequate amounts. Although the minimum therapeutic dose is not specifically determined, the usual recommended oral administration generally exceeds 10^9 CFU/day.⁵ Probiotics have well-established therapeutic efficacies against various gut disorders such as diarrhea, lactose intolerance, and inflammatory bowel diseases; recent findings suggest potential roles of probiotics in alleviating hypercholesterolemia, hypertension, and postmenopausal symptoms⁶ and in anticarcinogenesis.⁷ Various strains of species of lactobacilli and bifidobacteria have been identified as probiotics and incorporated into food products and supplements. However, the incorporation of the beneficial bacteria is often challenged with the preservation of viability during processing, storage, and gastrointestinal transit.⁸

Strategies to improve the stability of probiotics in food products include product fortification with probiotic substrate, pH adjustment, aseptic packaging, freeze-drying, and refrigerated storage.⁹ Encapsulation has also been applied to enhance the delivery of probiotics into the intestines¹⁰ and acts as a protective carrier, which is robust against processing conditions and gastrointestinal transit for selective release at targeted area such as the colon. Major challenges faced in bacterial encapsulation include (1) thermal insulation to preserve stability in heat-processed products and (2) suitable capsule size for optimal cell loading without compromising the textural and organoleptic properties of food products.¹¹ Microencapsulation involves carriers measuring several micrometers to 1 mm, whereas nanoencapsulation falls within submicrometer levels. Conventional microencapsulation such as spray-drying suffers from high mortality due to simultaneous dehydration and thermal inactivation.¹¹ Nanoencapsulation offers advantages such as immobilization efficiency due to increased surface area to volume ratio, robust protection due to flexibility in selection of encapsulant and its properties, and minimized sensorial effect when incorporated into food matrices due to the diminutive size. In addition, the amplified surface area to volume ratio in nanofibers may confer protection against heat processing due to reduced thermal conductivity with volume, as observed by Wu et al.¹²

Electrospinning is a nanofiber fabrication technique that applies high voltage to draw a polymer solution from a spinneret tip to a grounded collector. Upon charging, a jet of polymer solution emerges from the needle tip, forming a cone known as the Taylor cone, which breaks out into a jet when the critical voltage is achieved. The electrical potential between the tip and the grounded collector draws the jet in a whipping motion and

Received: March 8, 2011

Revised: June 29, 2011

Accepted: June 29, 2011

Published: June 29, 2011

stretches it into continuous fibers of nanosized diameter as a nonwoven mat on the grounded collector. Electrospinning has produced nanofibers from various synthetic and biopolymers for applications including tissue engineering and drug delivery.¹³ The size and properties of nanofibers can be designed to suit specific applications by modifying the parameters of the spinning process (voltage, spinning distance, flow rate) and those of the spinning solution (viscosity, conductivity, surface tension).¹⁴ Biopolymers that are biocompatible, biodegradable, and non-toxic are favored for nanoencapsulation of bioactives for food and biomedical applications aimed at immobilization, protection from adverse environments, and preservation of stability.⁸

Our previous research showed that agrowastes from oil palm and soybean contained dietary fibers that could be spun into nanofibers using electrospinning technology.¹⁵ The present study aimed to develop and evaluate agrowaste-based nanofibers as encapsulants of a probiotic, *Lactobacillus acidophilus*. To our knowledge, this is the first study to investigate the potential of agrowaste fibers as functional nanomaterials, which may provide some indications for a potential alternative encapsulation technique for the selected beneficial bacteria, *L. acidophilus*.

MATERIALS AND METHODS

Production of Nanofibers from OPT, OPF, and Okara.

Soluble dietary fiber (SDF) fractions from OPT, OPF, and okara were obtained as previously described.¹⁵ SDF solutions were amended with poly(vinyl alcohol) (PVA, average M_w 85,000–124,000, 87–89% hydrolyzed; Sigma-Aldrich, Steinheim, Germany) at a concentration of 8% (w/v) and stirred at 100 °C using a magnetic stirrer until complete dissolution. The spinning solutions from okara, OPT, and OPF were characterized by measuring the viscosity (A&D Vibro Viscometer SV-10, Tokyo, Japan), conductivity, and pH (Mettler Toledo S47 Seven-Multi dual meter pH/conductivity, Columbus, OH).

The solutions were autoclaved to achieve sterility and electrospun at 25 °C to produce nanofibers. The grounded collector was lined with aluminum foil to collect spun fibers. Electrospinning parameters were set as follows: flow rate, 0.1 mL/h; tip-collector distance, 15 cm; and voltage, 12 kV. The collected nanofibers were dried under vacuum (Binder VD, Tuttlingen, Germany) at 40 °C for 24 h and vacuum-packed until further analyses.

Characterization of Nanofibers. *Scanning Electron Microscopy (SEM).* The morphology of electrospun nanofibers were assessed using SEM. Samples were affixed to sample stubs and subsequently gold-coated using a Polaron SC515 SEM Coating System voating dystem (Bio-Rad sputter coater, Hemel Hempstead, U.K.). The samples were then viewed and photographed using a Leo Supra 50VP Ultrahigh Field Emission scanning electron microscope (FESEM; Carl Zeiss, Oberkochen, Germany). Fiber size distribution was determined using a desktop SEM (Phenom, Phenom-World, The Netherlands) complemented with Phenom ProSuite—Fibermetric software.

Attenuated Total Reflectance Infrared Spectroscopy (ATR-FTIR). The nanofibers were characterized using FTIR spectroscopy to study the chemical composition and bonding present. The ATR-FTIR spectra of nanofiber samples were recorded using the Thermo Nicolet Nexus FTIR spectrometer coupled with an ATR detector (Thermo Nicolet, Madison, WI). All spectra were recorded in the mid-IR region 4000–400 cm^{-1} at a resolution of 4 cm^{-1} with 32 scans. Analysis of the spectral data was performed by using OMNIC version 6.0 (Thermo Nicolet) software.

Thermal Characterization. Thermal characterization of nanofibers was performed using differential scanning calorimetry (DSC) and thermogravimetric analysis (TGA). Glass transition temperature (T_g) and

melting temperature (T_m) were determined using DSC (DSC-6, Perkin-Elmer, Waltham, MA). The nanofiber samples were heated from 40 to 400 °C at a heating rate of 10 °C/min in a nitrogen atmosphere. TGA of the electrospun nanofibers was performed using a thermal analyzer (Pyris 1 TGA, Perkin-Elmer). Samples were heated from 25 to 700 °C at a heating rate of 10 °C/min to investigate the weight loss behavior and degradation temperature.

Production of Nanofiber-Encapsulated *L. acidophilus*

FTDC 8933. *Preparation of Stained Bacterial Suspension.* *L. acidophilus* FTDC 8933 was obtained from the Culture Collection Centre of Universiti Sains Malaysia. The stock culture was stored at –20 °C in 40% (v/v) sterile glycerol. The cultures were activated three successive times in sterile de Mann, Rogosa, and Sharpe (MRS) broth (Hi-Media, Maharashtra, India) supplemented with 0.15% (w/v) filter-sterilized (0.45 μm) L-cysteine hydrochloride (MRS-LC, Hi-Media) prior to experimental use. Activated cells were cultured and collected by centrifugation at 2330g for 15 min at 4 °C, washed twice, and resuspended in phosphate-buffered saline (PBS, pH 7.4). The cells were stained with fluorescein diacetate (FDA) using the method described by Corich et al.¹⁶

The sterile spinning solutions were inoculated with the prepared cells and electrospun in the dark to preserve the fluorescing FDA dye. Some samples were collected on microscope slides for fluorescence microscopy imaging. Samples of *L. acidophilus* encapsulated in nanofibers from okara, OPT, and OPF were collected, vacuum-packed, and stored at 4 °C until further analyses.

Characterization of Nanofiber-Encapsulated *L. acidophilus*

*Viability of *L. acidophilus* FTDC 8933.* The viability of encapsulated cells was assessed using fluorescence microscopy. Nanofibers containing *L. acidophilus* that were collected on microscope slides were observed using an Olympus BH2 fluorescence microscope (Olympus Optical, Tokyo, Japan) fitted with a Progres C10+ Image Capture and VideoTest 5.0 image analysis system.

The viability of cells was also determined using the pour-plate assay. This was conducted to determine the viability of cells in the spinning solution prior to electrospinning, and the survival of cells upon encapsulation in nanofibers over a storage period of 21 days at 4 °C. Briefly, 1 mL of inoculated spinning solution was serially diluted, plated using MRS-LC agar (Hi-Media), and incubated at 37 °C. The viability of *L. acidophilus* FTDC 8933 in spinning solutions and encapsulated in nanofibers was determined as log(cfu/g) nanofibers. Nanofibers were weighed and dissolved in peptone at 25 °C to release the encapsulated cells, prior to serial dilutions and pour-plating. The viability assay was performed for samples at intervals of $t = 01$ (spinning solution) and $t = 0, 1, 3, 5, 7, 14,$ and 21 ($t =$ number of days stored at 4 °C).

Statistical Analysis. Data analysis was performed using SPSS Inc. software (version 15.0; Chicago, IL). One-way ANOVA was used to evaluate the significant differences between sample means, at a significance level of $\alpha = 0.05$. Mean comparisons were assessed by Tukey's test.

RESULTS AND DISCUSSION

Characterization of Spinning Solutions. The process of electrospinning can be manipulated by a number of variables including solution properties, such as conductivity, viscosity, and surface tension, and process parameters, such as voltage, tip-collector distance, and flow rate.¹⁴ Thus, the properties of different spinning solutions were measured to evaluate their influence on the diameter of nanofibers produced (Table 1). A spinning solution made from SDF of okara had a higher pH value ($P < 0.05$) at 5.39 ± 0.01 , followed by OPF and OPT. Although agrowastes were treated at pH 9 to yield SDF, the pH values of SDF decreased upon autoclaving. Our preliminary data ruled out the effect of PVA addition, as the pH of the PVA solution before

Table 1. Measurements of pH, Conductivity, and Viscosity of Spinning Solutions Prepared from Addition of Poly(vinyl alcohol) into Soluble Dietary Fiber (SDF) Fractions of Okara, Oil Palm Trunk (OPT), and Oil Palm Frond (OPF)^a

SDF	pH	conductivity (mS/cm)	viscosity (mPa·s)
okara	5.39 ± 0.01 A	8.51 ± 0.04 B	578.00 ± 11.02 A
OPT	4.60 ± 0.01 C	9.48 ± 0.03 A	168.00 ± 4.58 C
OPF	5.23 ± 0.01 B	7.85 ± 0.02 C	293.67 ± 13.50 B

^a Means in the same column with different letters are significantly different ($P < 0.05$).

autoclaving was 5.60 ± 0.01 , whereas after autoclaving it was 5.24 ± 0.01 . Thus, we believe that the reduction in pH was not contributed by any chemical interaction of PVA, but may be caused by autoclaving, which caused chemical degradation of the cellulose cell wall and the interaction of cellulose fibers with alkali.¹⁷ Depolymerization of cellulose produces a mixture of carboxylic and hydroxyl carboxylic acids, which leach into and reduce the pH of spinning solutions. The released cellulose degradation products tend to have strong metal-complexing ability in high-pH conditions, leading to displacement of carboxylic acid hydrogen ions by free metal ions in the solution, which further decrease the pH. Our previous study quantified various minerals in the agrowaste fiber materials including calcium and iron, which could leach into the SDF.¹⁵ Calcium is known to be present in high amounts due to its role in binding pectin and maintaining the integrity of cell walls.¹⁸ Carbohydrate-derived carboxylic acids have been studied as sequestering agents for calcium.¹⁹ The culmination of studies suggested the possibility of initial pH decrease from the release of carboxylic acids and minerals during treatment, followed by further pH decrease from complex formation between the degradation products and free mineral, leading to the drastic drop in pH from pH 9 before autoclaving to the range of 4.6–5.4 after alkali and heat treatment.

The lower pH (4.60 ± 0.01) and viscosity (168.00 ± 4.58 mPa·s) ($P < 0.05$) of SDF from OPT resulted in higher conductivity (9.48 ± 0.03 mS/cm) compared with SDF from OPF (7.85 ± 0.02 mS/cm) ($P < 0.05$). The viscosity of a solution dictates the mobility of the ions, thus directly influencing conductivity. The lower solution viscosity of OPT resulted in higher conductivity as compared with OPF, which possessed higher solution viscosity (293.67 ± 13.50 mPa·s), resulting in lower conductivity at 7.85 ± 0.02 ($P < 0.05$). Although the okara solution had higher viscosity (578.00 ± 11.02 mPa·s), the conductivity (8.51 ± 0.04 mS/cm) was higher compared with the OPF solution ($P < 0.05$). This could be due to a higher concentration of free ions from dissociation reaction which could have resulted in higher conductivity.²⁰ Son et al.²¹ noted that the conductivity of PVA solutions was also strongly dependent on the pH, with higher conductivities observed in low-pH regions. OPT with lower pH compared with OPF (5.23 ± 0.01) possessed higher conductivity ($P < 0.05$). Higher conductivities of okara (8.51 ± 0.04 mS/cm) and OPT in turn increased the charge densities of the spinning solution, thus imposing stronger elongation forces to eject jets under electric field, resulting in fibers with smaller diameters.²¹ As a result, the nanofibers spun from SDF of okara (Figure 1A) and OPT (Figure 1B) were observed to be finer than nanofibers spun from SDF of OPF (Figure 1C) under SEM.

The viscosities of spinning solutions, as controlled by polymer concentration, are important determiners of fiber size and morphology in the spinning of polymeric fibers.¹⁴ High solution viscosities present a predominant entanglement effect which, in turn, produce stable fiber jets.²² The SDF of okara had higher initial viscosity; thus, after the addition of PVA, it had a higher viscosity ($P < 0.05$) at 578.00 ± 11.02 mPa·s compared to SDF of OPT (168.00 ± 4.58 mPa·s) and OPF (293.67 ± 13.50 mPa·s). Our previous study also showed that okara possessed higher soluble dietary fiber content,¹⁵ which leached into the soluble fiber fraction during autoclaving, thus contributing to higher viscosity. Toda et al.²³ also showed that okara, which contains heat-extractable proteins and polysaccharides, increased the viscosity of soy milk processed with okara. The higher viscosity of SDF from okara also contributed to finer fiber size as observed under SEM (Figure 1).

Characterization of Nanofibers. *SEM.* The spinning solutions were successfully spun into nanofibers measuring 200–400 nm with generally uniform sizes (Figure 1). With the aim of producing smooth nanofibers with consistent diameters, preliminary electrospinning with lower concentrations of PVA produced defects such as beads and junctions (data not shown). Increasing the concentration of PVA to 8% (w/v) resulted in uniform, smooth, and bead-free nanofibers. Son et al.²¹ noted that the viscosity of solution rapidly increased with the addition of PVA beyond 7 wt %, which was the minimal concentration for a stabilized jet with consistent whipping and consequently forming long uniform PVA fibers, due to the onset of chain entanglement. Sufficient chain entanglement in spinning solution allows better spinning of continuous nanofibers.

Attenuated Total Reflectance Infrared Spectroscopy (ATR-FTIR). The molecular structure of electrospun agrowaste-based nanofibers was evaluated using ATR-FTIR, which is a powerful tool to study the conformational properties of polysaccharides and also the chemical constituents present in the nanofibers.^{8,24,25}

The ATR-FTIR spectra of okara, OPT, and OPF nanofibers corresponded to the spectrum of PVA nanofiber with major peaks related to the hydroxyl and acetate groups associated with neat PVA²⁶ (Figure 2). The large band between 3700 and 3000 cm^{-1} indicated O—H stretching from inter- and intramolecular hydrogen bonds.²⁵ The other major peak observed between 2935 and 2943 cm^{-1} was attributed to vibrational bands due to C—H stretching from alkyl groups in PVA, whereas the peak at 1733 cm^{-1} was assigned to the C=O and C—O stretching from residual acetate groups in the PVA matrix.²⁶ Another prominent peak at 1094 cm^{-1} represented the C—O stretching and O—H bending in PVA. An intense peak at 1648 cm^{-1} commonly associated with adsorbed water molecules in fibers²⁴ was notably absent in the spectra, suggesting the removal of water from nanofibers during electrospinning.

Apart from the chemical composition of PVA, peaks were also attributable to the soluble-fiber components in the spinning solution. The peak observed at 1732 cm^{-1} was indicative of acetyl and uronic ester groups of hemicelluloses. They can also be attributed to the carboxyl groups in the acids and esters of acetic, *p*-coumaric, ferulic, and uronic acids, which are the main constituents of extractives and hemicelluloses.²⁷ In addition, prominent peaks at 1427, 1375, and 1253 cm^{-1} represented C—H, O—H, or CH₂ bending,²⁴ whereas the peak at 1250 cm^{-1} can be assigned to C—O stretching vibrations of aliphatic primary and secondary alcohols associated with the hemicellulose material removed from insoluble fibers.²⁵

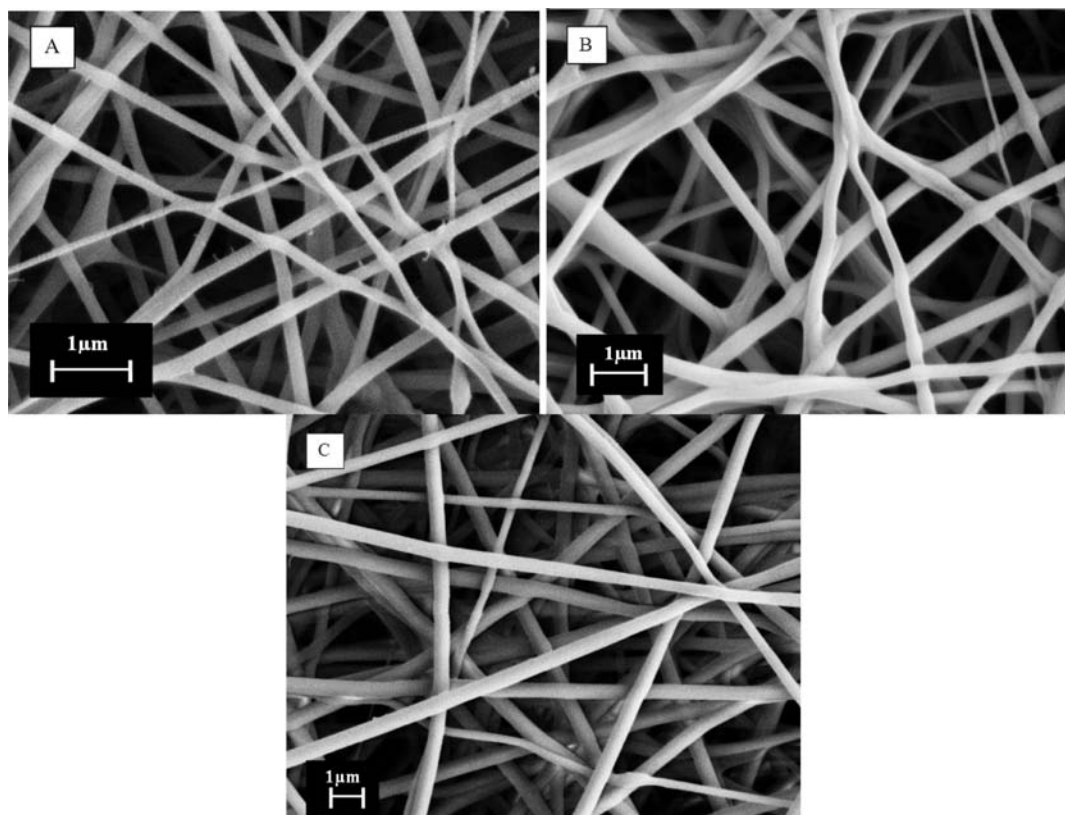


Figure 1. SEM micrographs of electrospun nanofibers from the soluble dietary fiber fraction of (A) okara, (B) oil palm trunk, and (C) oil palm frond.

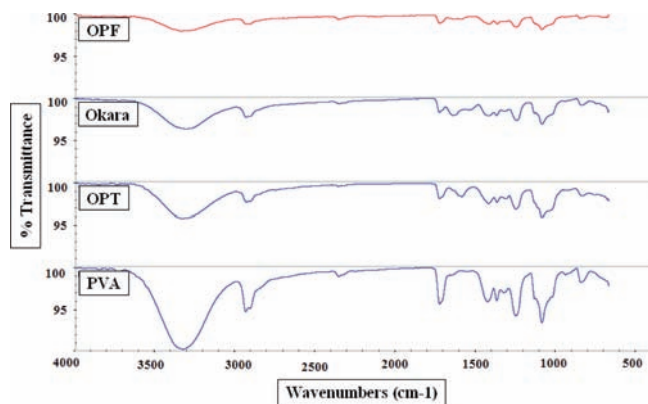


Figure 2. ATR-FTIR spectra of electrospun nanofibers from poly(vinyl alcohol) (PVA), okara, oil palm trunk (OPT), and oil palm frond (OPF).

Thermal Characterization. Thermogravimetric analysis (TGA) and differential scanning calorimetry (DSC) were used to thermally characterize the nanofibers. The weight loss of nanofibers as a function of degradation temperature was as shown in the TGA thermogram of the first-order derivatives (Figure 3). The thermogram of PVA nanofiber showed two regions of maximum weight loss, whereas nanofibers produced from soluble fibers with PVA additive showed three regions of major weight loss. The weight loss of the partially acetylated PVA nanofiber, at onset temperatures around 295 and 437 °C, corresponded to the release of acetyl groups that were transformed to acetic acid molecules with subsequent in situ chain stripping (295 °C), following which chain scission and

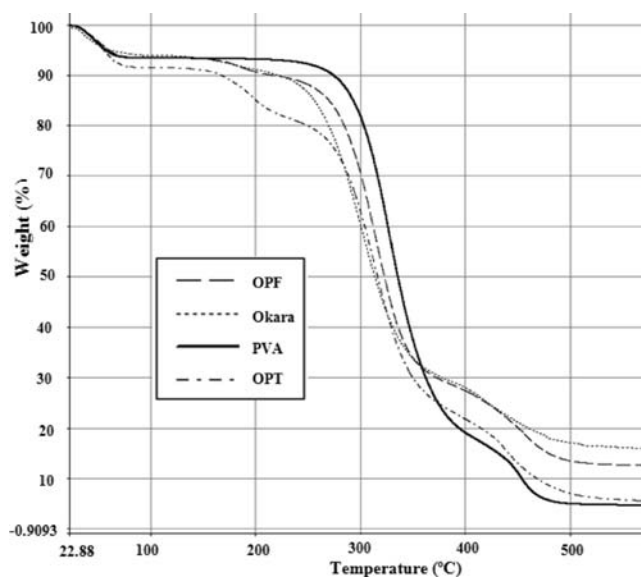


Figure 3. TGA thermogram of electrospun nanofibers from poly(vinyl alcohol) (PVA), okara, oil palm trunk (OPT), and oil palm frond (OPF).

decomposition (437 °C) occurred.²⁶ Peresin et al.²⁶ also noted that the electrospinning process did not affect the structure of the matrix polymer when thermograms of PVA before and after electrospinning were compared.

The agrowaste-based nanofibers with added PVA showed comparable thermograms. Thermogravimetric curves exhibited

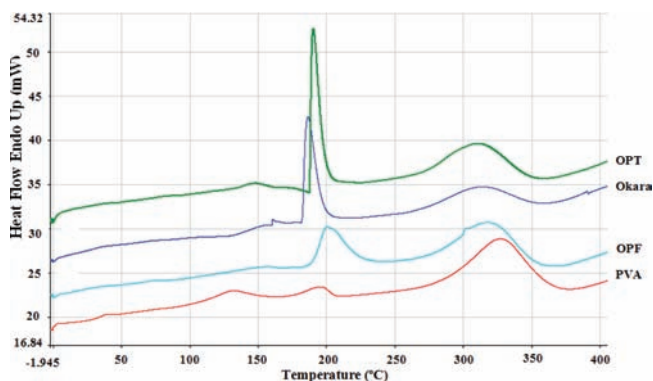


Figure 4. DSC thermogram of electrospun nanofibers from poly(vinyl alcohol) (PVA), okara, oil palm trunk (OPT), and oil palm frond (OPF).

first weight loss at 157 °C (okara nanofiber) and 164 °C (OPT and OPF nanofibers), due to loss of adsorbed water. Maximum weight loss was recorded at 273.1, 284.1, and 282.9 °C for nanofibers from okara, OPT, and OPF, respectively, attributable to the structural decomposition of the PVA side chain. This was followed by a third degradation point at 426.0, 425.0, and 427.9 °C for nanofibers from okara, OPT, and OPF, respectively, which accounted for the decomposition of the PVA main chain. The degradation temperatures of blend fibers were between the two temperatures of each material's onset of degradation, a trend that was also observed by Zhang et al.,²⁸ who evaluated PVA–soy blend nanofibers.

DSC curves of nanofibers (Figure 4) showed that the maximum peak corresponding to melting temperature was at 186.8–200.53 °C, with the higher melting enthalpy recorded for the OPT nanofiber at 183.7 J/g, whereas the lower melting enthalpy was at 37.3 J/g for the PVA nanofiber (Table 2). Because the spinning solutions were prepared with the addition of 8% PVA, nanofibers fabricated from agrowaste soluble fiber had greatly increased melting enthalpies, compared with nanofibers fabricated from plain PVA (dissolved in water). The degree of crystallinity (χ_c) calculated from the melting enthalpy was higher in nanofibers prepared from agrowaste soluble dietary fiber fractions (Table 2). Higher maxima of melting and melting enthalpy are indicative of more perfect molecular orientation and higher crystallinity, as more energy will be required to disrupt the higher molecular orientation.⁸ Thus, the addition of agrowaste solubilized fiber improved the crystallinity or molecular orientation in nanofibers, compared with plain PVA (dissolved in water). The high melting temperature of nanofibers indicated potential incorporation in heat-processed foods such as baked food, where it can remain stable at working temperatures of 50–180 °C.

Characterization of Nanofiber-Encapsulated *L. acidophilus*. SEM. The incorporation of *L. acidophilus* into spinning solutions resulted in beaded fiber morphology (Figure 5). The *L. acidophilus* cells were entirely enclosed within the nanofibers, forming local widening of the fiber that was almost spherical in shape, and were distributed along the nanofibers. The bacteria, which were initially dispersed in the polymer solution in random orientation, were gradually oriented along the stream lines due to sink-like flow at the Taylor cone.²⁹

In addition to SEM imaging, the presence of *L. acidophilus* was further supported by fluorescence microscopy images (Figure 6). FDA is a nonfluorogenic molecule that permeates cells to serve as

Table 2. DSC Maximum of Melting (T_m), Melting Enthalpy (ΔH_m), and Degree of Crystallinity (χ_c) of Electrospun Nanofibers from Okara, Oil Palm Trunk (OPT), Oil Palm Frond (OPF), and Poly(vinyl alcohol) (PVA)

nanofiber	T_m^a (°C)	ΔH_m^b (J/g)	χ_c^c
okara	186.30	167.90	1.21
OPT	190.46	183.70	1.32
OPF	200.53	126.30	0.91
PVA	195.40	37.30	0.27

^a T_m (°C) is the DSC maximum melting temperature. ^b ΔH_m (J/g) is the melting enthalpy. ^c $\chi_c = (\Delta H_m) / [(\Delta H_m^0 \times w)]$; ΔH_m^0 is the heat of fusion for the 100% crystalline polymer, estimated to be $\Delta H_m^0 = 139$ J/g;²⁶ w is the weight fraction of polymeric material in the respective composite.

a substrate for nonspecific esterases, leading to an activation of fluorescence.¹⁶ Hence, the presence and distribution of viable cells in nanofibers were observed as bright green fluorescence. The green fluorescence appeared within the beaded structures of PVA nanofibers, indicating the encapsulation of cells within the structures, which appears evenly distributed along the nanofibers.

The distribution of nanofiber sizes was also evaluated (Figure 5). Tubular nanofibers showed smaller diameter sizes, ranging from 229 to 272 nm, whereas bundles containing encapsulated probiotics presented a broader size distribution of 422–703 nm, with a high frequency of fibers measuring around 425 nm.

Viability of *L. acidophilus* FTDC 8933. We also evaluated the survivability of *L. acidophilus* upon electrospinning and its storage stability under refrigeration temperature (4 °C). The viability of *L. acidophilus* in spinning solution was also measured to compare the viability of the bacteria before and after electrospinning. The viability of electrospun nanofiber-encapsulated *L. acidophilus* generally decreased ($P < 0.05$) upon electrospinning (Table 3). Bacteria encapsulated in OPF nanofiber showed a higher survival percentage at 90%, followed by bacteria encapsulated in OPT and okara nanofibers at 85.3 and 78.6%, respectively. The decrease in probiotic viability after electrospinning can be attributed to a drastic change in the osmotic environment due to the rapid evaporation of water upon electrospinning.⁸ The sustained viability indicated the stability of the probiotic against high voltage and shear stress during electrospinning. Our results are comparable with nanoencapsulated *L. plantarum* in electrospun poly(ethylene oxide) nanofibers, which showed survival rates of 83.7% following the electrospinning process,³⁰ whereas other methods of preserving *L. acidophilus* such as freeze-drying revealed lower survivability of 72.85–73.88% after the freeze-drying process.³¹

The nanofiber-encapsulated probiotics were stored for evaluation of storage stability at 0, 1, 3, 5, 7, 14, and 21 days. The stability of the probiotic in OPF nanofiber was most prominent, retaining viable counts with no significant difference ($P < 0.05$) until day 14 and by the end of the study showed a survival of 72% (Table 3). OPT nanofiber retained 49% of bacterial viability by the end of the study, whereas okara nanofiber retained only 37.7% bacterial viability after 21 days.

The spinnability of the agrowaste soluble dietary fiber fraction and the properties of resulting nanofibers were complemented with the addition of PVA, a biocompatible hydrophilic polymer that can confer high oxygen barrier when dry, without affecting the bioactivity of bacteria.⁸ Freeze-dried *L. acidophilus* has been

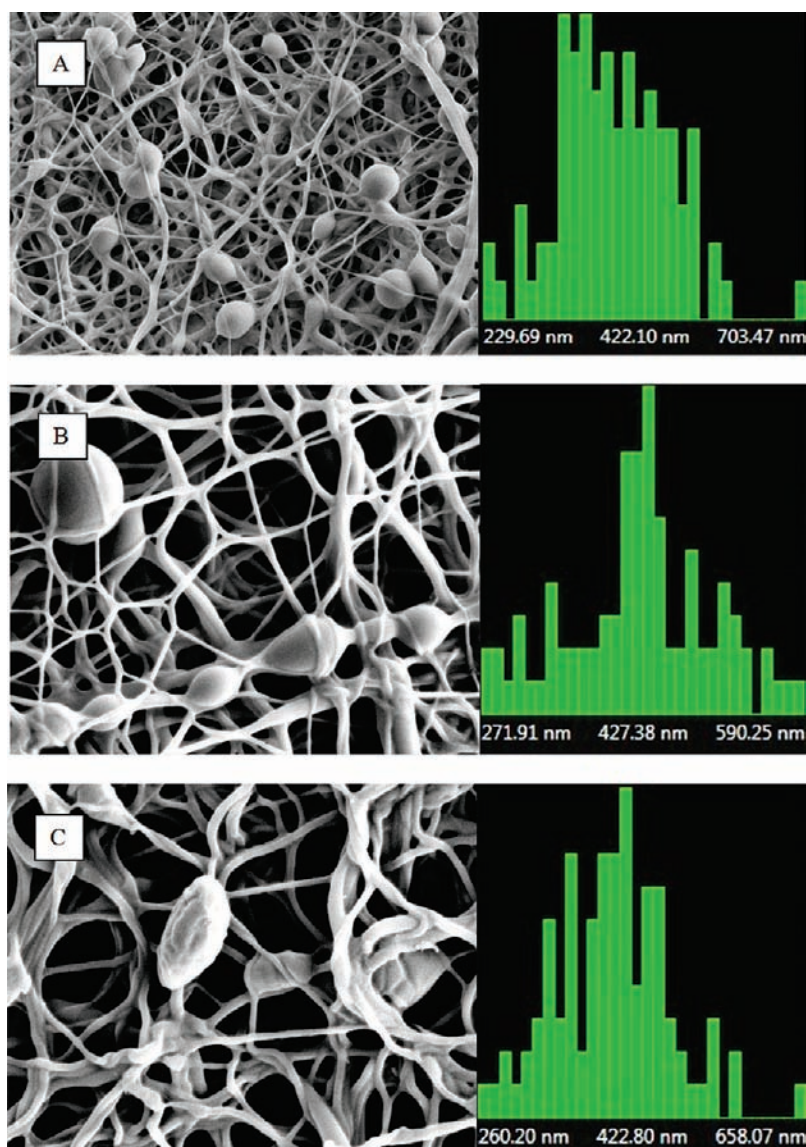


Figure 5. SEM micrographs and corresponding size distribution histograms of nanofibers containing *L. acidophilus* from (A) okara, (B) oil palm trunk (OPT), and (C) oil palm frond (OPF).

Table 3. Viability of *L. acidophilus* FTDC 8933 in Spinning Solutions ($t = 01$) and in Nanofibers from Okara, OPT, and OPF at Time Intervals $t = 0, 1, 3, 5, 7, 14,$ and 21 Days^a

nanofiber containing <i>L. acidophilus</i>	viability (log cfu/g)							
	spinning solution 01	time (days)						
		0	1	3	5	7	14	21
okara	9.56 ± 0.06 B,a	7.51 ± 0.18 B,b	7.23 ± 0.01 C,b	7.10 ± 0.03 C,b	5.12 ± 0.10 B,c	5.27 ± 0.08 B,c	3.90 ± 0.09 C,d	3.60 ± 0.21 C,d
OPT	11.01 ± 0.50 A,a	9.39 ± 0.09 A,b	9.14 ± 0.03 A,b	8.93 ± 0.04 B,b	8.72 ± 0.23 A,b	5.44 ± 0.11 B,d	6.73 ± 0.27 B,c	5.40 ± 0.05 B,d
OPF	9.91 ± 0.03 B,a	8.92 ± 0.02 A,b	8.80 ± 0.65 B,b	9.03 ± 0.02 A,b	8.72 ± 0.44 A,b	8.96 ± 0.03 A,b	7.96 ± 0.04 A,c	7.13 ± 0.04 A,d

^a Means in the same row with different lower case letters are significantly different ($P < 0.05$). Means in the same column with different upper case letters are significantly different ($P < 0.05$).

noted to lose stability and viability in the presence of elevated moisture content and oxygen level. Increased water activity decreased bacterial survival, whereas a reduced oxygen level improved

storage stability.³² Thus, the process of electrospinning, which completely removes the fiber solvent (water), and the protective nanofiber encapsulant, which excludes environmental oxygen,

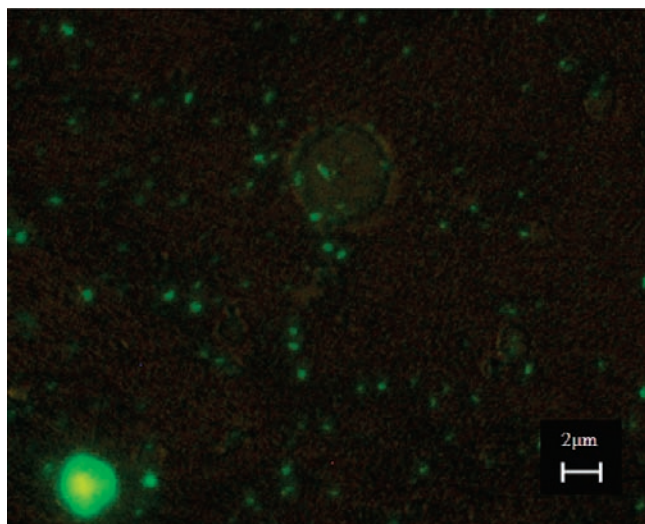


Figure 6. Optical micrograph of FDA-stained *L. acidophilus*-encapsulated within nanofibers electrospun from okara SDF solution. Fluorescence illumination revealed live bacteria within the fibers.

can contribute to the stability of *L. acidophilus*, possibly offering potential in extending the shelf life of probiotic products. In addition, the use of the agrowaste soluble fiber fraction as probiotic carrier may contribute to increased dietary fiber consumption in conjunction with probiotic encapsulation.

Nanoencapsulation of probiotics in nanofibers offers advantages in the incorporation of probiotics in food products, with reduced undesirable sensory effects, such as graininess or off-flavors often associated with consuming fibers, due to its minute size, and increased protection against heat treatment due to insulation properties, which are enhanced with decreasing fiber diameter.¹² Reduced fiber radius has been observed to reduce radiative heat flux or heat transfer via radiation through fiber insulations using electrospun superfine fibers.¹² Thus, probiotics encapsulated in electrospun nanofibers may have higher survival rates in thermal processing compared with microcarriers, presenting a potential of nanofibers for probiotic incorporation in heat-processed food, a long-standing challenge in bacteria encapsulation.

In summary, nanofibers were successfully produced from the soluble dietary fiber fractions of okara, OPT, and OPF. Thermal analysis suggested potential thermal protection of nanofibers for encapsulation of *L. acidophilus* in heat-processed food due to nanosize dimensions and high melting temperatures of at least 180 °C. Cells of *L. acidophilus* survived the electrospinning conditions of high shear stress and high voltage, retaining viability during storage at refrigeration temperature (4 °C). The flexibility of the electrospinning process in the modification of parameters may enable further improvements to increase the viability of encapsulated bacteria and serve as an alternative for bacterial protection. The agrowaste-based soluble dietary fiber fraction showed good potential as a nanoencapsulant for probiotics with concomitant supplementation of dietary fiber. Further research may be warranted to improvise nanofibers with controlled release properties for the controlled release of probiotics in the intestines, increased encapsulation efficiency, and probiotic stability while also evaluating the in vivo release and efficacy of nanoencapsulated probiotic.

AUTHOR INFORMATION

Corresponding Author

*E-mail: mintze.liong@usm.my. Phone: +604 653 2114. Fax: +604 657 3678.

Funding Sources

This project was supported by USM RU Grant 1001/PTE-KIND/811141 and USM RUPGRS Grant 1001/PFARMASI/843004. W.-Y.F. expresses her gratitude to the National Science Foundation Fellowship (Malaysia).

REFERENCES

- (1) Malaysian Palm Oil Board (MPOB). *World Oils and Fats*, 2009, <http://econ.mpob.gov.my/> (accessed Dec 2010).
- (2) Prestamo, G.; Rupérez, P.; Espinosa-Martos, I.; Villanueva, M.; Lasunción, M. The effects of okara on rat growth, cecal fermentation and serum lipids. *Euro. Food Res. Technol.* **2007**, *225* (5), 925–928.
- (3) Oliveira, L. S.; Franca, A. S. Chapter 11: From solid biowastes to liquid biofuels. In *Agricultural Wastes*; Ashworth, G. S., Azevedo, P., Eds.; Nova Science Publishers: Hauppauge, NY, 2009; pp 1–25.
- (4) Katayama, M.; Wilson, L. A. Utilization of okara, a byproduct from soymilk production, through the development of soy-based snack food. *J. Food Sci.* **2008**, *73* (3), S152–S157.
- (5) De Champs, C.; Maroncle, N.; Balestrino, D.; Rich, C.; Forestier, C. Persistence of colonization of intestinal mucosa by a probiotic strain, *Lactobacillus casei* subsp. *rhamnosus* Lcr35, after oral consumption. *J. Clin. Microbiol.* **2003**, *41* (3), 1270–1273.
- (6) Lye, H.-S.; Kuan, C. Y.; Ewe, J.-A.; Fung, W.-Y.; Liong, M.-T. The improvement of hypertension by probiotics: effects on cholesterol, diabetes, renin, and phytoestrogens. *Int. J. Mol. Sci.* **2009**, *10*, 3755–3775.
- (7) Commane, D.; Hughes, R.; Shortt, C.; Rowland, I. The potential mechanisms involved in the anti-carcinogenic action of probiotics. *Mutat. Res.* **2005**, *591* (1–2), 276–289.
- (8) Lopez-Rubio, A.; Sanchez, E.; Sanz, Y.; Lagaron, J. M. Encapsulation of living bifidobacteria in ultrathin PVOH electrospun fibers. *Biomacromolecules* **2009**, *10*, 2823–2829.
- (9) Knorr, D. Technology aspects related to microorganisms in functional foods. *Trends Food Sci. Technol.* **1998**, *9* (8–9), 295–306.
- (10) Meiners, J.-A. Micro-encapsulation of probiotics. In *Probiotics and Probiotics Science and Technology*; Charalampopoulos, D., Rastall, R. A., Eds.; Springer Science+Business Media: Heidelberg, NY, 2009; pp 805–823.
- (11) Anal, A. K.; Singh, H. Recent advances in microencapsulation of probiotics for industrial applications and targeted delivery. *Trends Food Sci. Technol.* **2007**, *18* (5), 240–251.
- (12) Wu, H.; Fan, J.; Qin, X.; Zhang, G. Thermal radiative properties of electrospun superfine fibrous PVA films. *Mater. Lett.* **2008**, *62* (6–7), 828–831.
- (13) Wang, H.-S.; Fu, G.-D.; Li, X.-S. Functional polymeric nanofibers from electrospinning. *Recent Patents Nanotechnol.* **2009**, *3*, 21–31.
- (14) Pham, Q. P.; Sharma, U.; Mikos, A. G. Electrospinning of polymeric nanofibers for tissue engineering applications: a review. *Tissue Eng.* **2006**, *12* (5), 1197–1211.
- (15) Fung, W.-Y.; Yuen, K.-H.; Liong, M.-T. Characterization of fibrous residues from agrowastes and the production of nanofibers. *J. Agric. Food Chem.* **2010**, *58* (13), 8077–8084.
- (16) Corich, V.; Soldati, E.; Giacomini, A. Optimization of fluorescence microscopy techniques for the detection of total and viable lactic acid bacteria in whey starter cultures. *Ann. Microbiol.* **2004**, *54* (3), 335–342.
- (17) Norkus, E.; Vaiciuniene, J.; Vuorinen, T.; Macalady, D. L. Equilibria of Cu(II) in alkaline suspensions of cellulose pulp. *Carbohydr. Polym.* **2004**, *55* (1), 47–55.
- (18) Adamsen, A. P. S.; Kin, D. E. A.; Rigsby, L. L. Chemical retting of flax straw under alkaline conditions. *Textile Res. J.* **2002**, *72* (9), 789–794.

(19) Bazin, H.; Bouchu, A.; Descotes, G.; Petit-Ramel, M. Comparison of calcium complexation of some carboxylic acids derived from D-glucose and D-fructose. *Can. J. Chem.* **1995**, *73*, 1338–1347.

(20) Dalmas, P. Conductivity measurement on pure water according to the recommendations of the USP Pharmacopoeia USP24-NF19. Radiometer Analytical S.A. International Laboratory News, 2000.

(21) Son, W. K.; Youk, J. H.; Lee, T. S.; Park, W. H. Effect of pH on electrospinning of poly(vinyl alcohol). *Mater. Lett.* **2005**, *59* (12), 1571–1575.

(22) Lee, G.-H.; Song, J.-C.; Yoon, K.-B. Controlled wall thickness and porosity of polymeric hollow nanofibers by coaxial electrospinning. *Macromol. Res.* **2010**, *18* (6), 571–576.

(23) Toda, K.; Chiba, K.; Ono, T. Effect of components extracted from okara on the physicochemical properties of soymilk and tofu texture. *J. Food Sci.* **2007**, *72* (2), C108–C113.

(24) Sain, M.; Panthapulakkal, S. Bioprocess preparation of wheat straw fibers and their characterization. *Ind. Crop Prod.* **2006**, *23*, 1–8.

(25) Cherian, B. M.; Pothen, L. A.; Nguyen-Chung, T.; Mennig, G.; Kottaisamy, M.; Thomas, S. A novel method for the synthesis of cellulose nanofibril whiskers from banana fibers and characterization. *J. Agric. Food Chem.* **2008**, *56* (14), 5617–5627.

(26) Peresin, M. S.; Habibi, Y.; Zoppe, J. O.; Pawlak, J. J.; Rojas, O. J. Nanofiber composites of poly(vinyl alcohol) and cellulose nanocrystals: manufacture and characterization. *Biomacromolecules* **2010**, *11* (3), 674–681.

(27) Alemdar, A.; Sain, M. Isolation and characterization of nanofibers from agricultural residues – wheat straw and soy hulls. *Bioresour. Technol.* **2008**, *99* (6), 1664–1671.

(28) Zhang, X. F.; Min, B. G.; Kumar, S. Solution spinning and characterization of poly(vinyl alcohol)/soybean protein blend fibers. *J. Appl. Polym. Sci.* **2003**, *90*, 716–721.

(29) Dror, Y.; Salalha, W.; Khalfin, R. L.; Cohen, Y.; Yarin, A. L.; Zussman, E. Carbon nanotubes embedded in oriented polymer nanofibers by electrospinning. *Langmuir* **2003**, *19* (7), 7012–7020.

(30) Heunis, T. D. J.; Botes, M.; Dicks, L. M. T. Encapsulation of *Lactobacillus plantarum* 423 and its bacteriocin in nanofibers probiotics and antimicrobial proteins. *Journal Title* **2010**, *2* (1), 46–51.

(31) Capela, P.; Hay, T. K. C.; Shah, N. P. Effect of cryoprotectants, prebiotics and microencapsulation on survival of probiotic organisms in yoghurt and freeze-dried yoghurt. *Food Res. Int.* **2006**, *39* (2), 203–211.

(32) Kurtmann, L.; Carlsen, C. U.; Risbo, J.; Skibsted, L. H. Storage stability of freeze-dried *Lactobacillus acidophilus* (La-5) in relation to water activity and presence of oxygen and ascorbate. *Cryobiology* **2009**, *58* (2), 175–180.